Science Translational Medicine AAAS

An osseointegrated human-machine gateway for long-term sensory feedback and motor control of artificial limbs

Max Ortiz-Catalan *et al.*

Sci Transl Med **6**, 257re6 (2014);
DOI: 10.1126/scitranslmed.3008933

Editor's Summary

A Bone-Anchored Arm Prosthetic

An artificial limb should not only anatomically resemble its original counterpart but also function and feel just like it. Currently available prosthetic limbs allow for basic functions ––closing a door or taking a step––but they often do not support fine-motor control or sensory perception. Ortiz-Catalan and coauthors describe a first-in-human trial of a bone-anchored (osseointegrated) upper-arm prosthetic that attached directly to the bone, nerves, and muscles of the remaining limb. The patient was followed for 1 year, demonstrating finer motor control (grasping, for example, an egg without breaking it) and a greater range of motion (touching toes and reaching arm overhead) compared with a conventional socket prosthesis with surface electrodes. Direct electrical stimulation of the peripheral nerves also provided the patient a sense of touch. The study was in only one patient, thus preventing quantification of improvement, which may vary depending on the amount of soft tissue and scar tissue remaining in the stump. Nevertheless, osseointegration could revolutionize the field of neuroprosthetics, giving patients more intuitive control and more freedom of movement.

NEUROPROSTHETICS

An osseointegrated human-machine gateway for long-term sensory feedback and motor control of artificial limbs

Max Ortiz-Catalan,[1,2]* Bo Håkansson,[1] Rickard Brånemark[2]

A major challenge since the invention of implantable devices has been a reliable and long-term stable transcutaneous communication. In the case of prosthetic limbs, existing neuromuscular interfaces have been unable to address this challenge and provide direct and intuitive neural control. Although prosthetic hardware and decoding algorithms are readily available, there is still a lack of appropriate and stable physiological signals for controlling the devices. We developed a percutaneous osseointegrated (bone-anchored) interface that allows for permanent and unlimited bidirectional communication with the human body. With this interface, an artificial limb can be chronically driven by implanted electrodes in the peripheral nerves and muscles of an amputee, outside of controlled environments and during activities of daily living, thus reducing disability and improving quality of life. We demonstrate in one subject, for more than 1 year, that implanted electrodes provide a more precise and reliable control than surface electrodes, regardless of limb position and environmental conditions, and with less effort. Furthermore, long-term stable myoelectric pattern recognition and appropriate sensory feedback elicited via neurostimulation was demonstrated. The opportunity to chronically record and stimulate the neuromuscular system allows for the implementation of intuitive control and naturally perceived sensory feedback, as well as opportunities for the prediction of complex limb motions and better understanding of sensory perception. The permanent bidirectional interface presented here is a critical step toward more natural limb replacement, by combining stable attachment with permanent and reliable human-machine communication.

INTRODUCTION

The functionality restored by powered limb prostheses has not improved considerably since their introduction in the 1960s, mostly owing to the lack of an intuitive control system deprived from sensory feedback. Open-loop myoelectric control via surface electrodes has been since then the most sophisticated control solution clinically available. Electromyography (EMG) recorded by electrodes on the skin (surface EMG) is limited to superficial muscles and susceptible to myoelectric crosstalk (interference), motion artifacts, and environmental conditions, mostly owing to the skin interface, and thus considerably degrading the controllability of the prostheses.

The ability to directly interface the neuromuscular system via implanted electrodes to provide intuitive control of artificial limbs has been pursued for decades. In 1977, implanted epimysial electrodes allowed a transradial amputee to simultaneously control two degrees of freedom (DoF). This pioneering attempt failed over time owing to infection in the percutaneous interface, which consisted of a lead penetrating the skin to reach an epidermal connector (*1*, *2*). Percutaneous leads were early identified with safety and reliability problems that compromise long-term stability (*1*–*4*). This is an important problem because without a long-term stable and reliable cutaneous gateway, a realistic clinical implementation is compromised, regardless of the sophistication of the neural interfaces.

As opposed to mechanically unstable leads, fixation via osseointegration enabled the first successful implantation of permanent percutaneous/permucosal devices (*5*). Dental, extraoral, and more sophisticated osseointegrated implants, such as bone-conducting devices, are currently used worldwide (*6*, *7*). A retrospective study of 1132 percutaneous bone-conducting devices displayed limited (4.5%) adverse soft-tissue reactions (*8*). The principle of osseointegration has been used for mechanically stable attachment of artificial limbs since 1990 (*9*), resulting in an improved quality of life (*10*–*12*) and self-perception (*13*). A recent prospective study on 51 patients with transfemoral amputation using the OPRA (Osseointegrated Prostheses for the Rehabilitation of Amputees) treatment reported a cumulative success rate of 92% at a 2-year follow-up (*10*).

Here, we show that by incorporating signal feedthrough mechanisms into the osseointegrated implant system, long-term bidirectional communication between the artificial limb and implanted neuromuscular interfaces is possible, thus improving controllability in comparison with surface electrodes and enabling sensory feedback, which is currently not provided by any limb prostheses (*14*).

RESULTS

The osseointegrated human-machine gateway

The standard OPRA implant system (Integrum) consists of two main components: (i) a fixture fully implanted in the intramedullary cavity of the bone at the stump, from which (ii) an abutment extends percutaneously to serve as the anchor for the prosthetic limb. The fixture and abutment are mechanically connected and secured by an abutment screw. The loads are directly transferred between the fixture and abutment (*10*).

To allow for bidirectional electrical communication, two feedthrough connectors were embedded in both ends of a custom-designed abutment screw. Similarly, a custom feedthrough connector was

[1]Division of Signal Processing and Biomedical Engineering, Department of Signals and Systems, Chalmers University of Technology, SE-412 96 Gothenburg, Sweden. [2]Center of Orthopaedic Osseointegration and Center of Advanced Reconstruction of Extremities, Department of Orthopaedics, Sahlgrenska University Hospital, University of Gothenburg, SE-431 80 Mölndal, Sweden.
*Corresponding author. E-mail: maxo@chalmers.se

embedded in the distal side of a central sealing component to mate the proximal connector embedded in the abutment screw (the standard abutment screw and central sealing components are solid pieces). Leads extend intramedullary from the central sealing component and then transcortically to a connector located outside the bone, where the electrodes' leads are interfaced (Fig. 1, A and B). The modular design of this osseointegrated human-machine gateway (OHMG) allows for easy and safe maintenance, which might be necessary, for example, to replace or upgrade electrodes without disturbing the osseointegrated implant and vice versa.

The critical parts of the OPRA implant system, namely, the osseointegrated and percutaneous components (fixture and abutment, respectively), as well as the implantation protocol and treatment of the skin interface, were kept unchanged, as in (*10*). These aspects were design priorities because the mechanically stable fixation provided by osseointegration and required for load transfer, and a stable skin interface for permanent cutaneous crossing, are key factors for a successful outcome of osseointegrated prostheses (*15*).

One patient with a trans-humeral amputation was the recipient of the OHMG system in January 2013 (Fig. 1B), which included one spiral cuff electrode and two bipolar and four monopolar epimysial electrodes (Fig. 1C). No complications were observed over 1-year implantation, and all components will remain implanted indefinitely. The patient reported no significant pain postoperatively or during the healing processes. A "pleasant" perception of phantom fingers 4 and 5 was reported immediately after the surgery, likely owing to the cuff electrode placed around the ulnar nerve.

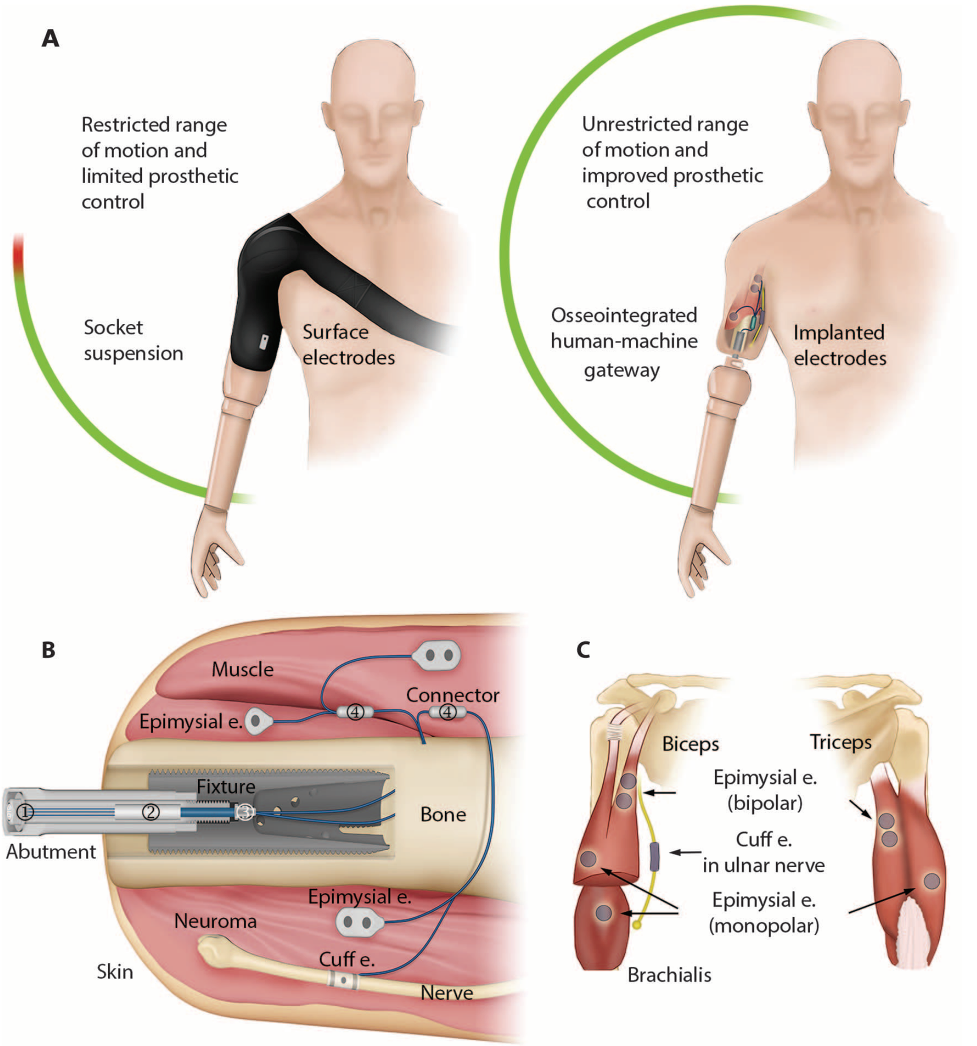

Fig. 1. Toward neural control of artificial limbs. (**A**) In the conventional socket suspension for high amputations, the adjacent joint is frequently constrained in the range of motion by the socket to provide sufficient suspension. The OHMG eliminates socket-related issues and allows for unrestricted limb motion (see movie S1). (**B**) The prosthetic limb was attached to the abutment, which transferred the load to the bone via the osseointegrated fixture. The abutment screw, which goes through the abutment to the fixture, was designed to maintain the abutment in place. A parallel connector (1) was embedded in the screw's distal end to electrically interface the artificial limb. This connector was electrically linked to a second feedthrough connector (2) embedded in the screw's proximal end. The stack connector (2) interfaced with a pin connector extending from the central sealing component (3), from which leads extended intramedullary and then transcortically to a final connector (4) located in the soft tissue. The leads from the neuromuscular electrodes ("e.") were mated to connector (4). (**C**) Placement of epimysial and cuff electrodes in the right upper arm.

Myoelectric control using implanted electrodes

Six weeks after the implantation of the OHMG, the patient was fitted with a custom-designed controller that used the bipolar epimysial electrodes as the new control source for his conventional myoelectric hand (contrary to surface electrodes). The new control system feed by epimysial EMG (eEMG) has been used in the patient's activities of daily living and at work (Fig. 2A), uninterrupted at the time of publication since March 2013. The controllability of the prosthesis is no longer restricted by limb position (movie S1) or affected by problems related to the skin interface, such as variations in impedance due to environmental conditions (cold and heat), as opposed to conventional prostheses using surface EMG (sEMG).

Previously, owing to the sensitivity of surface electrodes to myoelectric crosstalk, the prosthesis could not be operated while lifting the arm more than 80°. This is because the myoelectric activity of the shoulder muscles would actuate or block it (movie S1). Similarly, reaching far down would cause electrode displacement, thus making the prosthesis incontrollable. These impairments were no longer observed in the patient (movie S1 and fig. S1). Furthermore, the system was found to be resilient to motion artifacts and electromagnetic interference; no violent movements or electric noisy equipment

Fig. 2. Improved prosthetic control in daily living activities. (**A**) Patient performing daily living and professional activities using a myoelectric hand controlled using implanted electrodes via the OHMG. See movie S1 for more demonstrations. (**B**) Fold change of the EMG signal amplitude measured by the RMS. Data are means ± SD (n = 160). (**C**) The median frequency recorded by epimysial (eEMG) and surface (sEMG) electrodes at 3, 5, 7, and 8 months after implantation. Data are means ± SD (n = 160). See fig. S3 for examples of eEMG and sEMG signals. (**D** and **E**) Smallest actuation step achievable (in distance) (D) and gripping force (E) when using eEMG and sEMG as control source at 3, 5, and 7 months after implantation. Data are means ± SD (n = 30 per time point).

caused false activation (movie S1 and fig. S2), a well-known problem of surface electrodes (*16*).

The patient now reports less effort and higher controllability (survey available as Supplementary file "PatientSurvey.pdf"). The effort required to actuate the prosthesis was evaluated in relation to the maximal voluntary contraction (MVC). Contractions smaller than 15% MVC do not fatigue muscles, thus providing a relevant parameter in myoelectric control (*17*). The system was set to 12% (±2%) MVC, compared to the 60% (±5%) MVC previously required with sEMG. The patient reported no muscular fatigue, despite using his prosthesis 16 to 18 hours daily and occasionally wearing it during sleep. The time wearing the prosthesis increased by about 6 (±1) hours per day compared with sEMG, and phantom limb pain (PLP) was reduced by 40% (visual analog scale for pain), from "distressing" to sporadic "mild" episodes. This finding agrees with the known negative correlation between myoelectric prosthesis use and PLP (*18*).

The amplitude of the signals obtained from eEMG was considerably larger than surface recordings by an average of 6.9 ± 0.3– and 7.5 ± 0.4 (±SD)–fold for the biceps and triceps, respectively [root mean square (RMS), mV] (Fig. 2B). The difference between the biceps and triceps can possibly be explained by the thicker subcutaneous fat normally found over the triceps, which attenuates the myoelectric signals (*17*). The difference in amplitude was measured at MVC in four sessions from the 3rd to 8th month after implantation, along with electrode impedance. The latter exhibited little variability, confirming that the encapsulation period had ended and that the electrode-tissue interface was stable at 1.6 ± 0.06 kilohms. The difference in median frequency at a steady MVC was 45 and 88 Hz for eEMG versus sEMG for the biceps and triceps, respectively (Fig. 2C). The difference is not surprising, because the layers of soft tissue likely act as a spatial low-pass filter. An example of sEMG and eEMG signals is shown in fig. S3.

The grip resolution was evaluated by comparing the minimum possible actuation step, which was smaller when using eEMG from the biceps and triceps (Fig. 2D and movie S1). A considerable difference between eEMG and sEMG was found in the generation of a minimal incremental gripping force because this task requires a more controlled activation signal (Fig. 2E). The patient was aware of this improved resolution, allowing him to trust his prosthesis in handling smaller or more delicate objects, such as eggs, which he claims he did not attempt to grasp previously with the surface electrodes.

Myoelectric pattern recognition

We have previously demonstrated the possibility to predict distal motions using myoelectric pattern recognition (MPR) at the stump level, in spite of muscles directly responsible for such motions no longer being present (*19*). In the current clinical implementation, high-density sEMG (HD-sEMG) was used to facilitate the selection of suitable sites (Fig. 1C) that allowed MPR of eight motions (hand opening/closing, wrist pronation/supination, wrist flexion/extension, and elbow flexion/extension) with an accuracy of 94.3% (σ = 1.6%; n = 100). These sites became the implantation location for the epimysial electrodes, which postoperatively achieved 95.4% (σ = 1%; n = 100) accuracy.

With the same number of electrodes, eEMG thus yielded discrimination accuracy similar to that of sEMG (Fig. 3A). Furthermore, near-perfect discrimination was reached with eEMG after three training sessions (99.4%, σ = 0.5%). The accuracy was computed by dividing the number of absolute correct predictions (all classes in the true condition) by the number of absolute predictions. Traditional global accuracy (true conditions over the total of individual predictions) is generally larger and less informative in MPR. The global accuracy in this case was 98.7% (σ = 0.4%), 99.0% (σ = 0.2%), and 99.9% (σ = 0.1%) for surface preoperative, epimysial postoperative untrained, and epimysial postoperative trained, respectively.

We proceeded to evaluate the real-time controllability of three DoF currently provided by available commercial prosthetic devices (movie S2). The patient practiced a natural manipulation (as in the intact biological limb) of an electric hand, wrist rotator, and elbow (Fig. 3B), as well as their virtual equivalent in augmented reality (Fig. 3C) during three daily sessions. After the last session, a quantitative real-time

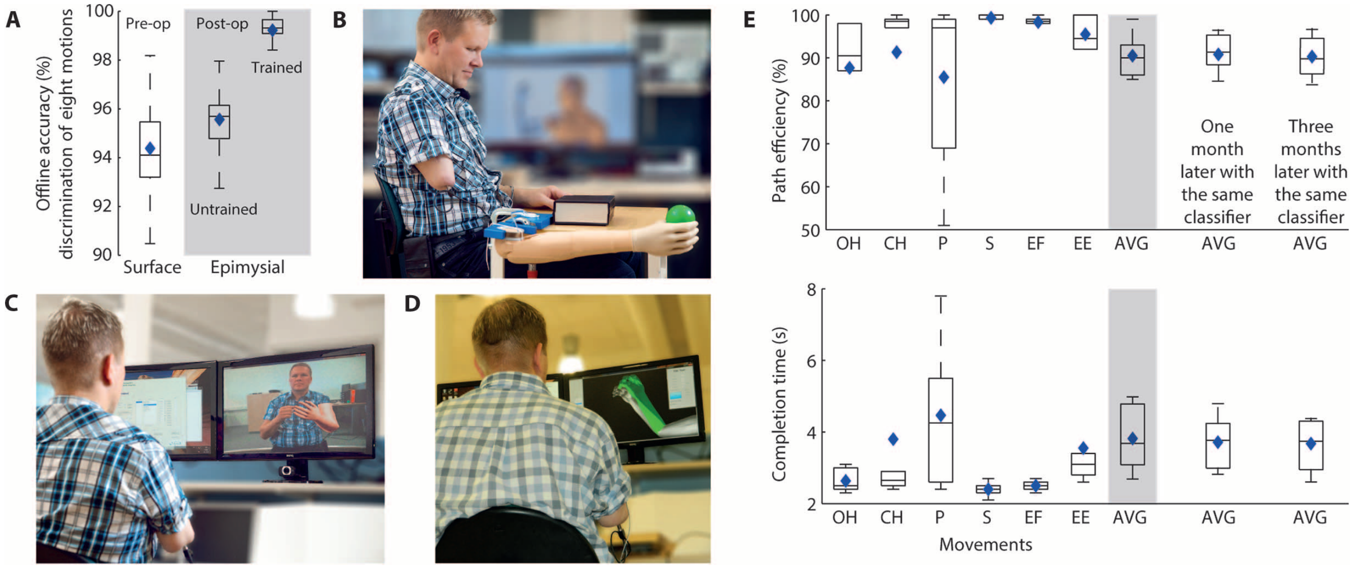

Fig. 3. Limb control based on MPR. (**A**) Offline accuracy reached in the MPR of eight motions—open hand, closed hand, pronation, supination, elbow flexion, elbow extension, wrist flexion, and wrist extension—using surface electrodes preoperatively (Pre-op) and epimysial electrodes postoperatively (Post-op) without training and after three training sessions (n = 121 feature vectors per motion). (**B** and **C**) The patient intuitively controlled a multifunctional prosthesis and a virtual limb in augmented reality through MPR, which was fed using permanently implanted electrodes (background blurred for clarity). (**D**) The patient performed real-time controllability tasks. See movie S2 for examples of performance in (B) to (D). (**E**) Real-time metrics of the path efficiency and completion time are shown for six motions (six trails each). These motions were selected because they are available in commercially prostheses (movie S2): open hand (OH), closed hand (CH), pronation (P), supination (S), elbow flexion (EF), and elbow extension (EE). AVG represents the average for all motions. The classifier was retested 1 and 3 months later. Box plots in (A) and (D) represent the 25th and 75th percentiles, with whiskers extending to the outliers. The dividing line is the median, and the mean is represented by a diamond mark.

evaluation was performed whereby a target limb posture must be reached by a virtual limb under the patient's control within a given time and range (*20*, *21*) (Fig. 3D and movie S2). As shown in movie S2 and Fig. 3E, high controllability was achieved with a completion rate of 100% over 36 attempts and average path efficiency of 90.5% (σ = 5.1%) in 3.8 s (σ = 0.9 s). These results are comparable to tests performed in able bodies [93.5% (σ = 13.9%) path efficiency reported in (*21*)] despite the absence of muscles directly responsible for some of the movements, such as hand opening/closing.

When retested for the hand and wrist only, the path efficiency was 96.3% (σ = 8%) in 3.0 s (σ = 1.0 s), over 24 attempts with 100% completion rate. Because a short training was allowed (three sessions), further improvement is expected with additional learning (*19*). Furthermore, an advantage of this approach over conventional MPR using sEMG is that the latter requires constant retraining owing to variations in the skin interface. Here, we demonstrate that an MPR controller retained similar performance for over 3 months if fed by implanted electrodes (Fig. 3E). No retraining was performed between the sessions.

Sensory feedback

One principal goal for prosthetic feedback is to mimic the natural mechanoreceptors to produce appropriate and distally referred tactile perception. The feasibility of artificially providing somatosensory information through neurostimulation has been limited to short-term (<4 weeks) studies (*3*, *22*–*24*), aside from an early prosthetic implementation in 1974 (*25*), and a more recent study describing 6 weeks of reproducible perception in a patient 18 months after amputation using extraneural electrodes and percutaneous leads (*26*). We report in this study that repeatedly similar tactile perception (quality, magnitude, and localized projection) can be chronically reproduced (11 months) through direct electrical stimulation of the peripheral nerves despite long-term amputation (>10 years).

A single active charge-balanced biphasic pulse was delivered with increasing current until the patient reported perception (stimulation threshold). The smallest projected field, described as "superficial tapping with the tip of a pen," was electrode-specific (Fig. 4, A and B) and reproducible within the same day (morning and afternoon), on five consecutive days (in the 7th month), and over 11 months (Fig. 4C). The perceived dimension and quality coincided with intraneural microstimulation (INMS) studies (*27*). At the stimulation threshold, the patient was able to discriminate individual pulses up to 8 to 10 Hz [10 Hz found in INMS (*27*)], and a "tingling" sensation was reported above 20 Hz. Mixed results were obtained between 10 and 19 Hz, where the patient reported fewer pulses than actually given and most commonly a "tingling" sensation. This behavior has been associated with rapid adaptive fibers (*27*). The projected field could be extended by either increasing the current of single pulses by 30 to 50 μA or using pulse trains at frequencies above 20 Hz. The level of intensity was reported to rise with increasing frequency in steps of 7 to 10 Hz.

DISCUSSION

The results here support the notion that implanted electrodes improve controllability and eliminate the long-term stability problems associated with their surface counterpart, such as environmental dependency and susceptibility to crosstalk interference and motion artifacts. These problems are major obstacles for the clinical implementation of MPR

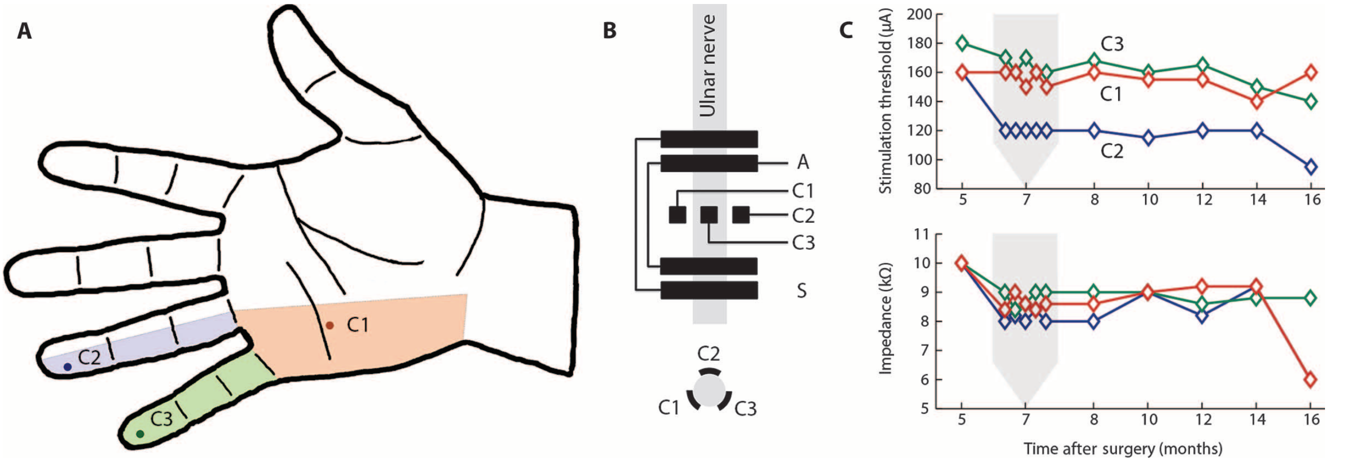

Fig. 4. Tactile perception via neurostimulation. (**A**) The dark points represent the electrode-specific projected field repeatedly reported (over 11 months) for a single pulse at stimulation threshold. (**B**) Electrode contact distribution around the ulnar nerve. A, anode; C, cathode; S, screen to reduce extraneural interference during recordings. (**C**) Stimulation threshold and impedance of each electrode over time. The data points represent the measurements taken two times per day (morning and afternoon). In the 7th month after implantation, measurements were taken in five consecutive days.

controllers, as attempted since the 1970s using sEMG (*28*, *29*). No long-term implementation of MPR has been reported despite the availability of prosthetic hardware. Off-the-shelf myoelectric prosthetic components can be combined to restore up to three DoF; however, owing to the limited control currently available via conventional surface electrodes, which requires cumbersome switching protocols, patients are rarely fitted with several myoelectrically controlled DoF.

Inherent to surface electrodes is the separation to the source of information (muscles) by layers of soft tissue, fat, and skin. This increases the crosstalk from neighboring muscles and rapidly reduces the EMG signals by about two orders of magnitude over the first 7 mm (*30*). Being close to the source, as with epimysial electrodes, is of particular importance for the operation of myoelectric prostheses, which use threshold values to discriminate between volitional EMG and background noise (including myoelectric crosstalk). A higher threshold requires a stronger muscular contraction and reduces the speed/force range in proportional controllers. Recordings with the bipolar epimysial electrodes (used for the controller) showed no myoelectric crosstalk, as opposed to recordings with the monopolar epimysial (fig. S1), which yielded a higher amplitude for the signal of interest (as expected from a wider differential measurement). Despite the fact that myoelectric crosstalk is observable in the monopolar electrodes, it can be argued that because the signal-to-noise ratio is preserved, similar operational performance in direct control could be achieved with either bipolar or monopolar epimysial electrodes.

The patient described in this study showed stability of an osseointegrated interface over the course of 18 months. A limitation of this case study is that only one patient has been treated with the proposed technology. Therefore, the precise improvements on controllability cannot be generalized, because these will vary depending on the amount of soft and scar tissue present in the stump. Nevertheless, we presume that the independence to environmental factors and limb position, as well as the resilience to motion artifacts and electromagnetic interferences, will be reproducible in the future across subjects, as it is inherent to the system.

Another limitation is that the MPR strategy here presented, which uses muscle synergies to predict motion intention, will be clinically relevant only if it is sufficiently robust for use in activities of daily living. This should be a subject of future work. Nevertheless, if combined with surgical techniques, such as targeted muscle reinnervation (*31*) or regenerative peripheral nerve interfaces (*32*), additional myoelectric sites can be made available to reliably and independently control several DoF.

A potentially more robust alternative to the use of muscle synergies for restoring the missing DoF is to directly interface the peripheral nerves to obtain physiologically appropriate control information. Similar to the report in (*1*), we did not observe clear motor neural activity, likely because the myelinated motor fibers had degenerated owing to the lack of a target muscle for 10 years (after amputation). However, acute studies using intrafascicular electrodes have suggested that motor nerve fibers remain viable in long-term amputees despite cortical reorganization and axotomy-induced degeneration (*3*, *22*). As opposed to cuff electrodes that mostly detect thick myelinated fibers close to the epineurium, intrafascicular electrodes have a higher sensitivity down to thin unmyelinated axons. We hypothesize that long-term use of physiologically appropriate control signals, as in the MPR controller presented here, could potentially induce the buildup of myelin in the related motor fibers to the point at which their activity can be measured extraneurally by the cuff electrode. This hypothesis is based on the finding that neural firing induces myelination (*33*). Such a long-term study has not been previously possible owing to the limitations on permanent implantation of neuromuscular interfaces in amputees. Nevertheless, in the case that extraneural cuff electrodes could not be successfully used for recording of motor activity, the modular design of the OHMG easily allows for upgrades to more selective neural interfaces, such as intrafascicular (*3*, *22*–*24*) or flat nerve interface electrodes (*26*). The current design of the OHMG allows communication for up to 12 independent signals, which is sufficient for the direct control (one-for-one) of few powered prosthetic units (for example, elbow, wrist, and hand). However, the number of electrodes can be considerably increased to thousands by implanting the acquisition electronics and using the OHMG for power supply and serial communication of the digitalized signals.

The patient requested that the amplifier gain be decreased 1 month after the first fitting, arguing that the hand was "too easy" to actuate.

The patient was not comfortable with operation requiring less than about 10% MVC. The problem was not related to false activations but to activation before perception of the controlling contraction. The patient reported that it is easier to control the hand while perceiving a certain degree of muscular effort, thus stressing the importance of sensory feedback. In this regard and despite the preliminary nature of the results presented on sensory feedback, these serve to demonstrate that tactile perception can be chronically reproduced, modulated, and thus potentially implemented in activities of daily living via the introduced bidirectional interface.

In sum, we have developed a clinically viable solution that addresses two major issues in the field of artificial limbs: stable attachment and natural control. The ultimate contribution of this work resides in enabling neuromuscular interfaces to become clinically relevant, thus paving the way for increased functionality, reduced disability, and better quality of life for patients with missing limbs.

MATERIALS AND METHODS

Study design

One patient was implanted with the OHMG to demonstrate its long-term stability and clinical relevance by allowing the use of implanted electrodes in the control of powered prostheses in activities of daily living. The experiments and clinical implementation were approved by the Västra Götalandsregionen ethical committee (Dnr: 769-12), and informed consent was obtained from the patient before the initiation of any experiment.

PLP and prosthetic use were assessed on three occasions using the short-form McGill Pain Questionnaire at 2 months before implantation and at 10 and 16 months after implantation (see Supplementary file "PatientSurvey.pdf"). Prosthetic control resolution by surface and epimysial electrodes was compared in three sessions (3, 5, and 7 months after implantation) by actuating, in the smallest possible step, the full range of operation (n = 30 trials per time point). The required percentage of MVC for the prosthesis operation was compared in the last session by comfortably actuating the prosthesis. The difference between sEMG and eEMG was measured in four sessions (3, 5, 7, and 8 months after implantation, n = 40 trials per time point). Offline MPR was assessed at three points in time with a recording session (121 feature vectors extracted per movement) as in (*34*): before implantation (2 days), after implantation (3 months), and after implantation after three training sessions (8 months). Real-time MPR performance was assessed as in (*21*) at the latter session and then 1 and 3 months later without additional training in between (six trails per movement). The stimulation threshold for perception was investigated two times, morning and afternoon (5, 7, 8, 10, 12, 14, and 16 months after implantation), and in five consecutive days in the 7th month after implantation.

Clinical implementation

The patient was implanted with the OHMG on 29 January 2013. The surgery was conducted at the Centre of Orthopaedic Osseointegration, Sahlgrenska University Hospital, Mölndal, Sweden. The recipient had undergone a trans-humeral amputation owing to a malignant tumor in 2003 and was treated with a custom-designed implant based on the standard OPRA design in 2009 using a two-stage surgical procedure and rehabilitation, as described elsewhere (*35*). The patient had been an active prosthetic user, wearing a myoelectric hand 10 to 12 hours daily.

Surgery was performed under general anesthesia and antibiotic prophylaxis. The abutment and abutment screw were replaced with the new custom-designed components. A skin incision was made laterally and medially, respectively, to expose muscles and nerves. A 3-mm hole was drilled at an angle of about 45° to the long axis of the bone. The intramedullary leads were routed through the skeleton proximally by fluoroscopic guidance. The muscle electrodes were implanted on the triceps, biceps, and brachialis, and their function was checked peroperatively. A nerve cuff electrode was placed around the ulnar nerve (see below). The wound was closed in layers. No postoperative complication was observed.

Electrode selection and placement

The superficial electrodes used for the HD-sEMG and to compare epimysial recordings (amplitude, frequency, and MPR) were individual, self-adhesive, and disposable Ag/AgCl of 1-cm diameter (GS26, Bio-Medical Instruments). These pre-gelled electrodes provide a higher signal quality than the dry electrodes used in conventional myoelectric prostheses and therefore provide an advantageous case for superficial recordings.

Magnetic resonance imaging was used preoperatively to evaluate the internal anatomy of the stump and to estimate suitable implantable component dimensions. The selection of appropriate locations for electrode placement was facilitated by HD-sEMG, which identified the locations with the strongest myoelectric activity and the weakest interference from shoulder muscles. This process was conducted for full shoulder abduction and flexion. Matrices of 9 × 4 electrodes were placed over biceps and triceps muscles (2-cm interelectrode distance, electrodes described above). From the eight epimysial electrode contacts available for implantation, four were used as bipolar for elbow flexion/extension to secure conventional myoelectric control (Fig. 1C). The remaining four contacts were distributed in three locations with the forth as a common differential. The location was decided by asking the patient to execute hand open/close, wrist flexion/extension, and wrist pronation/supination, and then an exhaustive search was used to select three electrodes that produced the highest MPR accuracy. (MPR is described in Supplementary Methods.)

Bipolar epimysial electrodes were sutured along the fibers on the short head of the bicep muscle and the long head of the triceps muscle (Fig. 1C). Monopolar epimysial electrodes were placed on the long head of the biceps, the lateral head of the triceps, and the brachialis muscles. The reference electrode common for the aforementioned monopolars was placed in electrically silent distal tissue, close to the abutment in the medial side (not shown in Fig. 1C). A cuff electrode was placed around the ulnar nerve about 10 cm from the terminal neuroma.

The epimysial and self-sizing spiral cuff electrodes (Ardiem Medical) were chosen for their proven safety during long-term use in human clinical applications (*16*, *36*–*39*). The arrangement of the contacts within the cuff (Fig. 4B) was based on previous work in which we found that a mixed configuration of ring and discrete contacts produces the highest signal-to-noise ratio while increasing the number of sites from which neural information can be retrieved within the same cuff (*40*). Furthermore, discrete contacts provide additional possibilities for selective stimulation.

Data analysis

The RMS and median frequency values of the myoelectric signals were calculated in segments of 200 ms with an overlap of 20 ms (n = 50).

The MPR accuracy was the average of a 100-fold cross-validation randomizing the extracted feature vectors in training, validation, and testing sets as described in (*34*). Descriptive statistics were used in this study to report variability, and no data were discarded as outliers.

SUPPLEMENTARY MATERIALS

www.sciencetranslationalmedicine.org/cgi/content/full/6/257/257re6/DC1
Methods
Fig. S1. Example of the eEMG resilience to myoelectric interference.
Fig. S2. Example of the eEMG resilience to motion artifacts.
Fig. S3. Examples of eEMG and sEMG signals in the human triceps.
Movie S1. Myoelectric control using epimysial versus surface electrodes.
Movie S2. Prosthetic control based on MPR.
File "PatientSurvey.pdf" (short-form McGill Pain Questionnaires).
References (*41*, *42*)

REFERENCES AND NOTES

1. R. B. Stein, D. Charles, J. A. Hoffer, J. Arsenault, L. A. Davis, S. Moorman, B. Moss, New approaches for the control of powered prostheses particularly by high-level amputees. *Bull. Prosthet. Res.* **10-33**, 51–62 (1980).
2. J. A. Hoffer, G. E. Loeb, Implantable electrical and mechanical interfaces with nerve and muscle. *Ann. Biomed. Eng.* **8**, 351–360 (1980).
3. G. S. Dhillon, S. M. Lawrence, D. T. Hutchinson, K. W. Horch, Residual function in peripheral nerve stumps of amputees: Implications for neural control of artificial limbs. *J. Hand. Surg. Am.* **29**, 605–615 (2004).
4. D. J. Weber, R. Friesen, L. E. Miller, Interfacing the somatosensory system to restore touch and proprioception: Essential considerations. *J. Mot. Behav.* **44**, 403–418 (2012).
5. P. I. Brånemark, B. O. Hansson, R. Adell, U. Breine, J. Lindström, O. Hallén, A. Ohman, Osseointegrated implants in the treatment of the edentulous jaw. Experience from a 10-year period. *Scand. J. Plast. Reconstr. Surg. Suppl.* **16**, 1–132 (1977).
6. R. Brånemark, P. I. Brånemark, B. Rydevik, R. R. Myers, Osseointegration in skeletal reconstruction and rehabilitation: A review. *J. Rehabil. Res. Dev.* **38**, 175–181 (2001).
7. A. F. Snik, E. A. Mylanus, D. W. Proops, J. F. Wolfaardt, W. E. Hodgetts, T. Somers, J. K. Niparko, J. J. Wazen, O. Sterkers, C. W. Cremers, A. Tjellström, Consensus statements on the BAHA system: Where do we stand at present? *Ann. Otol. Rhinol. Laryngol. Suppl.* **195**, 2–12 (2005).
8. C. A. Dun, H. T. Faber, M. J. de Wolf, E. A. Mylanus, C. W. Cremers, M. K. Hol, Assessment of more than 1,000 implanted percutaneous bone conduction devices: Skin reactions and implant survival. *Otol. Neurotol.* **33**, 192–198 (2012).
9. K. Hagberg, R. Brånemark, One hundred patients treated with osseointegrated transfemoral amputation prostheses—Rehabilitation perspective. *J. Rehabil. Res. Dev.* **46**, 331–344 (2009).
10. R. Brånemark, Ö. Berlin, K. Hagberg, P. Bergh, B. Gunterberg, B. Rydevik, A novel osseointegrated, percutaneous prosthetic system for treatment of patients with transfemoral amputation: A prospective study of 51 patients. *Bone Joint J.* **96-B**, 106–113 (2014).
11. J. Sullivan, M. Uden, K. P. Robinson, S. Sooriakumaran, Rehabilitation of the trans-femoral amputee with an osseointegrated prosthesis: The United Kingdom experience. *Prosthet. Orthot. Int.* **27**, 114–120 (2003).
12. K. Hagberg, R. Brånemark, B. Gunterberg, B. Rydevik, Osseointegrated trans-femoral amputation prostheses: Prospective results of general and condition-specific quality of life in 18 patients at 2-year follow-up. *Prosthet. Orthot. Int.* **32**, 29–41 (2008).
13. M. Lundberg, K. Hagberg, J. Bullington, My prosthesis as a part of me: A qualitative analysis of living with an osseointegrated prosthetic limb. *Prosthet. Orthot. Int.* **35**, 207–214 (2011).
14. C. Antfolk, M. D'Alonzo, B. Rosén, G. Lundborg, F. Sebelius, C. Cipriani, Sensory feedback in upper limb prosthetics. *Expert Rev. Med. Devices* **10**, 45–54 (2013).
15. K. Affeld, J. Grosshauser, L. Goubergrits, U. Kertzscher, Percutaneous devices: A review of applications, problems and possible solutions. *Expert Rev. Med. Devices* **9**, 389–399 (2012).
16. M. Ortiz-Catalan, R. Brånemark, B. Håkansson, J. Delbeke, On the viability of implantable electrodes for the natural control of artificial limbs: Review and discussion. *Biomed. Eng. Online* **11**, 33 (2012).
17. T. Kuiken, M. M. Lowery, N. S. Stoykov, The effect of subcutaneous fat on myoelectric signal amplitude and cross-talk. *Prosthet. Orthot. Int.* **27**, 48–54 (2003).
18. M. Lotze, W. Grodd, N. Birbaumer, M. Erb, E. Huse, H. Flor, Does use of a myoelectric prosthesis prevent cortical reorganization and phantom limb pain? *Nat. Neurosci.* **2**, 501–502 (1999).
19. M. Ortiz-Catalan, N. Sander, M. B. Kristoffersen, B. Håkansson, R. Brånemark, Treatment of phantom limb pain (PLP) based on augmented reality and gaming controlled by myoelectric pattern recognition: A case study of a chronic PLP. *Front. Neurosci.* **8**, 24 (2014).
20. A. M. Simon, L. J. Hargrove, B. A. Lock, T. A. Kuiken, Target Achievement Control Test: Evaluating real-time myoelectric pattern-recognition control of multifunctional upper-limb prostheses. *J. Rehabil. Res. Dev.* **48**, 619–627 (2011).
21. M. Ortiz-Catalan, B. Håkansson, R. Brånemark, Real-time and simultaneous control of artificial limbs based on pattern recognition algorithms. *IEEE Trans. Neural. Syst. Rehabil. Eng.* **22**, 756–764 (2014).
22. G. S. Dhillon, K. W. Horch, Direct neural sensory feedback and control of a prosthetic arm. *IEEE Trans. Neural Syst. Rehabil. Eng.* **13**, 468–472 (2005).
23. K. Horch, S. Meek, T. G. Taylor, D. T. Hutchinson, Object discrimination with an artificial hand using electrical stimulation of peripheral tactile and proprioceptive pathways with intrafascicular electrodes. *IEEE Trans. Neural Syst. Rehabil. Eng.* **19**, 483–489 (2011).
24. S. Raspopovic, M. Capogrosso, F. M. Petrini, M. Bonizzato, J. Rigosa, G. Di Pino, J. Carpaneto, M. Controzzi, T. Boretius, E. Fernandez, G. Granata, C. M. Oddo, L. Citi, A. L. Ciancio, C. Cipriani, M. C. Carrozza, W. Jensen, E. Guglielmelli, T. Stieglitz, P. M. Rossini, S. Micera, Restoring natural sensory feedback in real-time bidirectional hand prostheses. *Sci. Transl. Med.* **6**, 222ra19 (2014).
25. F. W. Clippinger, R. Avery, B. Titus, A sensory feedback system for an upper-limb amputation prosthesis. *Bull. Prosthet. Res.* **Fall**, 247–258 (1974).
26. D. Tan, M. Schiefer, M. W. Keith, R. Anderson, D. J. Tyler, in *6th Annual International IEEE/EMBS Conference on Neural Engineering, San Diego, CA, 6 to 8 November 2013* (IEEE, San Diego, CA, 2013), pp. 859–862.
27. J. Ochoa, E. Torebjörk, Sensations evoked by intraneural microstimulation of single mechanoreceptor units innervating the human hand. *J. Physiol.* **342**, 633–654 (1983).
28. P. Herberts, C. Almström, K. Caine, Clinical application study of multifunctional prosthetic hands. *J. Bone Joint Surg. Br.* **60-B**, 552–560 (1978).
29. R. W. Wirta, D. R. Taylor, F. R. Finley, Pattern-recognition arm prosthesis: A historical perspective—A final report. *Bull. Prosthet. Res.* **Fall**, 8–35 (1978).
30. J. H. Blok, D. F. Stegeman, A. van Oosterom, Three-layer volume conductor model and software package for applications in surface electromyography. *Ann. Biomed. Eng.* **30**, 566–577 (2002).
31. T. A. Kuiken, G. Li, B. A. Lock, R. D. Lipschutz, L. A. Miller, K. A. Stubblefield, K. B. Englehart, Targeted muscle reinnervation for real-time myoelectric control of multifunction artificial arms. *JAMA* **301**, 619–628 (2009).
32. T. A. Kung, N. B. Langhals, D. C. Martin, P. J. Johnson, P. S. Cederna, M. G. Urbanchek, Regenerative peripheral nerve interface viability and signal transduction with an implanted electrode. *Plast. Reconstr. Surg.* **133**, 1380–1394 (2014).
33. R. D. Fields, Myelination: An overlooked mechanism of synaptic plasticity? *Neuroscientist* **11**, 528–531 (2005).
34. M. Ortiz-Catalan, R. Brånemark, B. Håkansson, BioPatRec: A modular research platform for the control of artificial limbs based on pattern recognition algorithms. *Source Code Biol. Med.* **8**, 11 (2013).
35. S. Jönsson, K. Caine-Winterberger, R. Brånemark, Osseointegration amputation prostheses on the upper limbs: Methods, prosthetics and rehabilitation. *Prosthet. Orthot. Int.* **35**, 190–200 (2011).
36. K. L. Kilgore, P. H. Peckham, M. W. Keith, F. W. Montague, R. L. Hart, M. M. Gazdik, A. M. Bryden, S. A. Snyder, T. G. Stage, Durability of implanted electrodes and leads in an upper-limb neuroprosthesis. *J. Rehabil. Res. Dev.* **40**, 457–468 (2003).
37. X. Navarro, T. B. Krueger, N. Lago, S. Micera, T. Stieglitz, P. Dario, A critical review of interfaces with the peripheral nervous system for the control of neuroprostheses and hybrid bionic systems. *J. Peripher. Nerv. Syst.* **10**, 229–258 (2005).
38. J. Delbeke, Electrodes and chronic optic nerve stimulation. *Biocybern. Biomed. Eng.* **31**, 81–94 (2011).
39. K. H. Polasek, H. A. Hoyen, M. W. Keith, R. F. Kirsch, D. J. Tyler, Stimulation stability and selectivity of chronically implanted multicontact nerve cuff electrodes in the human upper extremity. *IEEE Trans. Neural. Syst. Rehabil. Eng.* **17**, 428–437 (2009).
40. M. Ortiz-Catalan, J. Marin-Millan, J. Delbeke, B. Håkansson, R. Brånemark, Effect on signal-to-noise ratio of splitting the continuous contacts of cuff electrodes into smaller recording areas. *J. Neuroeng. Rehabil.* **10**, 22 (2013).
41. M. Ortiz-Catalan, BioPatRec, http://code.google.com/p/biopatrec [accessed January 2014].
42. D. Andreu, D. Guiraud, G. Souquet, A distributed architecture for activating the peripheral nervous system. *J. Neural. Eng.* **6**, 026001 (2009).

Acknowledgments: We thank J. Lamkiewicz for his contribution to the implant's prototyping and manufacturing methods, O. Aszmann for his participation during the surgery, J. Delbeke for his insights on neural interfaces and comments on the manuscript, J. Wessberg for the discussion on artificial sensory feedback, S. Jönsson for the discussion on prosthetic components, J. Kalmar for facilitating the multifunctional prosthesis, B. R. Johansson for arranging resources for anatomical dissection, and P. Kvarnström for the schematic illustrations. **Funding:** This project was funded by Vinnova, Västra Götalandsregionen via Avtal om Läkarutbildning och Forskning, Consejo Nacional de Ciencia y Tecnología, Integrum AB, and Promobilia. **Author contributions:** M.O.-C. developed the MPR system, bioelectric amplifiers, and electronic controllers; designed and

performed the experiments; and drafted the manuscript. R.B. performed the surgical implementation. M.O.-C. and R.B. designed the implanted system. B.H. and R.B. supervised all the work realized in this project. All authors discussed the results and commented on the manuscript. **Competing interests:** M.O.-C. was partially funded by and R.B. is a stakeholder of Integrum, a medical device company developing bone-anchored prostheses. M.O.-C. and R.B. are inventors in a patent application (pending) concerning the implant system. B.H. declares no competing financial interests. **Data and materials availability:** The algorithms used for MPR are available in the open-source platform BioPatRec at https://code.google.com/p/biopatrec.

Submitted 28 February 2014
Accepted 7 July 2014
Published 8 October 2014
10.1126/scitranslmed.3008933

Citation: M. Ortiz-Catalan, B. Håkansson, R. Brånemark, An osseointegrated human-machine gateway for long-term sensory feedback and motor control of artificial limbs. *Sci. Transl. Med.* **6**, 257re6 (2014).